Sortase A as a tool for high-yield histatin cyclization

Jan G. M. Bolscher,[*,1,2] Menno J. Oudhoff,[*,2,3] Kamran Nazmi,[*] John M. Antos,[‡]
Carla P. Guimaraes,[‡] Eric Spooner,[‡] Evan F. Haney,[||] Juan J. Garcia Vallejo,[†]
Hans J. Vogel,[||] Wim van 't Hof,[*] Hidde L. Ploegh,[‡,§] and Enno C. I. Veerman[*]

[*]Department of Oral Biochemistry, Academic Centre for Dentistry Amsterdam, University of
Amsterdam and Vrije Universiteit (VU) Amsterdam, and the [†]Department of Molecular Cell Biology
and Immunology, VU Medical Center, Amsterdam, The Netherlands; [‡]Whitehead Institute for
Biomedical Research and [§]Department of Biology, Massachusetts Institute of Technology,
Cambridge, Massachusetts, USA; and [||]Biochemistry Research Group, Department of Biological
Sciences, University of Calgary, Calgary, Alberta, Canada

ABSTRACT   Cyclic peptides are highly valued tools in biomedical research. In many cases, they show higher receptor affinity, enhanced biological activity, and improved serum stability. Technical difficulties in producing cyclic peptides, especially larger ones, in appreciable yields have precluded a prolific use in biomedical research. Here, we describe a novel and efficient cyclization method that uses the peptidyl-transferase activity of the *Staphylococcus aureus* enzyme sortase A to cyclize linear synthetic precursor peptides. As a model, we used histatin 1, a 38-mer salivary peptide with motogenic activity. Chemical cyclization of histatin 1 resulted in $\leq$3% yields, whereas sortase-mediated cyclization provided a yield of >90%. The sortase-cyclized peptide displayed a maximum wound closure activity at 10 nM, whereas the linear peptide displayed maximal activity at 10 µM. Circular dichroism and NMR spectroscopic analysis of the linear and cyclic peptide in solution showed no evidence for conformational changes, suggesting that structural differences due to cyclization only became manifest when these peptides were located in the binding domain of the receptor. The sortase-based cyclization technology provides a general method for easy and efficient manufacturing of large cyclic peptides.—Bolscher, J. G. M., Oudhoff, M. J., Nazmi, K., Antos, J. M., Guimaraes, C. P., Spooner, E., Haney, E. F., Garcia-Vallejo, J. J., Vogel, H. J., van 't Hof, W., Ploegh, H. L., Veerman. E. C. I. Sortase A as a tool for high-yield histatin cyclization. *FASEB J.* 25, 2650–2658 (2011). www.fasebj.org

Key Words: intramolecular transpeptidation · wound closure stimulating peptide

NATURAL AND SYNTHETIC cyclic peptides have been subject of numerous studies in recent years (1). In medicinal chemistry, the imposition of conformational restraint through cyclization is a standard but difficult strategy to increase receptor affinity and/or selectivity of peptide ligands. Peptide cyclization has also been used to improve the activity and serum stability of antimicrobial peptides (2).

The human salivary peptide histatin 1 (Hst1), which accelerates reepithelization in simple and complex wound models (3, 4), is an example of a linear peptide of which the molar activity increases >1000-fold on cyclization. The low yield of cyclic Hst1 achieved with organic chemical ligation (<3%) has hampered more detailed mechanistic studies and has impeded analysis of the bioactive conformation using circular dichroism (CD) and NMR, methods that require relatively large amounts of peptide. We therefore sought a more efficient method of preparing cyclic histatin variants.

Sortase A (SrtA) from *Staphylococcus aureus* is a versatile bioengineering tool for modification of proteins by enzymatic ligation (5, 6). This includes site-specific derivatization of proteins (7, 8) with an array of functional groups, *e.g.*, fluorophores and photoaffinity labels. In addition, sortase has been used for the production of fusion proteins or cyclic proteins (9, 10). SrtA recognizes substrates that contain the sortase recognition motif LPETG, which is then cleaved between Thr and Gly, with the concurrent formation of a covalent acyl-enzyme intermediate, resolved by nucleophilic attack by a suitably exposed primary amine, such as the α-NH$_2$ group of an N-terminal Gly. Peptides that contain both the C-terminal LPETG motif and an N-terminal acceptor Gly residue may thus be cyclized by SrtA. In this study, we have developed a semienzymatic method, based on the intramolecular transpeptidase activity of sortase, for high-yield synthesis of cyclic peptides, using histatin as model peptide. Like the fully chemically cyclized Hst1, the sortase-cyclized Hst1 displayed a 1000-fold higher molar activity than its linear counterparts.

MATERIALS AND METHODS

Solid-phase peptide synthesis

Linear peptides (**Table 1**) were manufactured by solid-phase peptide synthesis using 9-fluorenylmethoxycarbonyl (Fmoc) chemistry with a MilliGen 9050 synthesizer (MilliGen/Biosearch, Bedford, MA, USA) according to the manufacturer's procedures. Peptide synthesis-grade solvents were used directly as obtained from Biosolve (Valkenswaard, The Netherlands). The N-α-Fmoc amino acids were obtained from Orpegen Pharma (Heidelberg, Germany). For Hst1, preloaded solid-phase resin [Fmoc-L-Asn(Trt)-PEG-PS, 0.1 mmol, loading 0.16 mmol/g; Applied Biosystems, Foster City, CA, USA] in 1-methyl-2-pyrrolidone (NMP) was applied to the column and equilibrated at a flow rate of 4 ml/min. Fmoc was removed with piperidine (20% v/v) in NMP for 6 min. Fmoc amino acids were dissolved at 4 times molar excess in N,N-dimethylformamide (DMF) containing 0.6 mM 2-(^{1}H-benzotriazole-1-yl)-1,1,3,3-tetramethyluronium tetrafluoroborate and 0.6 mM 1-hydroxybenzotriazole (HObt) and coupled in the presence of 0.45 mM N,N-diisopropylethylamine (DIPEA) in NMP by recycling for 1.5 h. Washings between the reaction steps were carried out with NMP. Subsequently, the peptide was detached from the resin and deprotected with 14 ml trifluoroacetic acid (TFA)/phenol/thioanisole/H_2O (85:5: 5:5) in a 25-ml syringe equipped with a frit, under gentle shaking for ≥2 h. Next, N_2 was flushed through the reaction mixture to reduce the volume to <2 ml. The reaction mixture was purged into 30 ml ice-cold diethylether in a 50-ml tube, followed by 2 washings of the resin with 2 ml TFA. The precipitated peptide was washed 4 times with ice-cold diethylether using a magnetically driven centrifuge (RVC 2-25; Christ, Osterode, Germany) at 230 g for 5 min, dissolved in 10 ml H_2O, flushed with N_2 to remove excess diethylether, and lyophilized.

Peptide purification

Peptides were purified by semipreparative RP-HPLC (Jasco Corp., Tokyo, Japan) on a Vydac C18-column (218MS510; Vydac, Hesperia, CA, USA). Peptides were dissolved in H_2O containing 5% acetonitrile (AcN; Biosolve) and 0.1% TFA. Elution was performed with a linear gradient from 15 to 45% AcN containing 0.1% TFA in 20 min at a flow rate of 4 ml/min. The absorbance of the column effluent was monitored at 214 nm, and peak fractions were pooled and lyophilized. Reanalysis by RP-HPLC on an analytic Vydac C18-column (218MS54) developed with a similar gradient at a flow rate of 1 ml/min revealed a purity of ≥95%. The authenticity was routinely confirmed by mass spectrometry (MS). Mass spectra were recorded with a Thermo LTQ ion-trap mass spectrometer in nanospray configuration (Thermo Fisher Scientific, Hampton, NH, USA) or a Microflex LRF matrix-assisted laser desorption/ionization time-of-flight (MALDI-TOF) mass spectrometer equipped with an additional gridless reflectron (Bruker Daltonik, Bremen, Germany).

Organic chemical cyclization

Glutamic acid at position 4 of Hst1 was used as starting point for synthesis of the linear peptide using an orthogonally protected Fmoc-Glu(Wang-resin)-ODmab (NovaBiochem, Läufelfingen, Switzerland), which allowed on-resin head-to-tail ligation. After completion of the discontinuous sequence (K^5-N^{38})(D^1-E^4), the N-terminal Fmoc was removed with 20% piperidine in NMP, and subsequently the C-terminal ODmab was removed by 2% hydrazine in DMF. On-resin head-to-tail cyclizations were achieved by prolonged reaction (72 h) with 1 eq benzotriazole-1-yl-oxytripyrrolidinophosphonium hexafluorophosphate (Biosolve), 1 eq HObt, and 1 eq DIPEA in DMF containing 20% dimethyl sulfoxide (DMSO; Biosolve) and 2% dichloromethane (DCM; Biosolve). After cleavage from the resins and purification by RP-HPLC, cyclization was confirmed by MALDI-TOF MS, which showed that the molecular mass of cHst1 was 4830 Da, 18 Da less than that of the linear Hst1. The overall yield was between 1 and 3%.

Expression and purification of SrtA

A soluble version of SrtA was created comprising the catalytic domain of the *S. aureus* SrtA (aa 26 to 206) and a hexahistidine tag at the N terminus (cloned in to pQE30; Qiagen, Valenica, CA, USA; ref. 11). Briefly, the SrtA-expression plasmid containing *Escherichia coli* BL-21 (DE3) was cultured in the presence of ampicillin (10 μg/ml) until OD_{600} ~ 0.7. SrtA production was induced by the addition of 1 mM isopropyl β-D-thiogalactopyranoside (IPTG). After an additional 3 h of culturing, bacteria were harvested by centrifugation at 3500 g at 4°C for 30 min and resuspended in ice-cold lysis buffer (50 mM Tris-HCl, pH 7.5, containing 150 mM NaCl, 20 mM imidazole, and 10% glycerol). Bacteria were lysed by passing through a prechilled cell disruption press (One Shot Model; Constant Systems Ltd., Daventry Northants, UK) operating at 1250 kpsi (8618 MPa). The lysate was cleared by centrifugation at 14,000 g at 4°C for 30 min. The supernatants were subjected to affinity chromatography on a recharged Ni^{2+}-HisTrap HP column (GE Healthcare, Uppsala, Sweden). The column was washed extensively with lysis buffer containing 50 mM imidazole and eluted with lysis buffer containing 500 mM imidazole. The imidazole was

TABLE 1. *Peptide sequences*

Peptide	Sequence
Linear	
Hst1	DSHEKRHHGYRRKFHEKHHSHREFPFYGDYGSNYLYDN
K-E(Hst1)[a]	KRHHGYRRKFHEKHHSHREFPFYGDYGSNYLYDN-DSHE
GG-Hst1-LPETGG	GGDSHEKRHHGYRRKFHEKHHSHREFPFYGDYGSNYLYDNLPETGG[b]
Cyclic	
cHst[c]	~DSHEKRHHGYRRKFHEKHHSHREFPFYGDYGSNYLYDN~
cGG-Hst1-LPET[d]	~GGDSHEKRHHGYRRKFHEKHHSHREFPFYGDYGSNYLYDNLPET~
Biotinylated cyclic	
cGG-Hst1-LPET_biotin[e]	~GGDSHEKRHHGYRRKFHEKHHSHREFPFYGDYGSNYLYDNLPET~

[a]Discontinuous sequence of Hst1 used for chemical cyclization. [b]Sortase recognition motifs: cleavage motif, amino acids underscored at right; acceptor motif, amino acids underscored at left. [c]Chemically cyclized Hst1. [d]Sortase-mediated cyclized Hst1. [e]K at position 17 (double underscored) was prelabeled with biotin.

removed by a buffer exchange step on a PD-10 desalting column (GE Healthcare). Purity was analyzed by SDS-PAGE; if necessary, affinity purification was repeated. The affinity-purified SrtA was stored in 10% glycerol, 50 mM Tris-HCl (pH 8.0), and 150 mM NaCl at $-80°C$ until further use.

Alternatively, SrtA was purified directly from the HisTrap elution fractions, without buffer changes or imidazole removal, by semipreparative RP-HPLC, using a linear gradient from 25 to 45% AcN containing 0.1% TFA in 20 min at a flow rate of 4 ml/min. HPLC-purified SrtA was lyophilized and stored at $-20°C$. The latter method produced SrtA of >95% purity.

Sortase-catalyzed cyclization and purification of cyclic peptides and SrtA

Linear peptides were equipped with the SrtA optimal cleavage site LPETGG (12, 13) at the C terminus (Table 1). A diglycine motif (GG) was appended at the N terminus, which served as a highly efficient acceptor allowing intramolecular ligation by a peptide bond. These peptides were synthesized on the solid-phase Fmoc-Gly-PEG-PS resin (0.1 mmol, loading 0.19 mmol/g; Applied Biosystems), processed, and purified as described above. The intramolecular transpeptidation reactions were conducted with 150 μM of the linear peptide and 50 μM SrtA in sortase reaction buffer (50 mM Tris, pH 7.5, containing 150 mM NaCl and 10 mM $CaCl_2$) at 37°C until cyclization was completed, as indicated by a peak shift in the RP-HPLC elution profile, using an analytic C18 column (218MS54; Vydac) developed with a gradient from 30 to 45% AcN in 20 min at a flow rate of 1 ml/min. The reaction mixture was subsequently separated by semipreparative RP-HPLC on a Vydac C18 column (218MS510), eluted with a gradient from 25 to 40% AcN containing 0.1% TFA in 20 min at a flow rate of 4 ml/min. This resulted in separation of the cyclic peptide from the linear starting material and SrtA. Peak fractions containing the cyclic peptide and SrtA, respectively, were pooled, lyophilized, and stored as dry powder at $-20°C$. Mass spectra of the fractions were performed on a Micromass LCT mass spectrometer (Micromass MS Technologies; Waters Corp., Milford, MA, USA) and a Paradigm MG4 HPLC system equipped with an HTC PAL autosampler (Michrom BioResources, Auburn, CA, USA) and a Waters symmetry 5 μm C8 column (2.1×50 mm), using $MeCN:H_2O$ (0.1% formic acid) as mobile phase and a flow rate of 150 μl/min or on a Microflex LRF MALDI-TOF, equipped with a gridless reflectron (Bruker Daltonik).

Determination of SrtA activity

SrtA activity was monitored using a FRET bacterial sortase substrate I (14), being LPETG equipped with the fluorophore EDANS at the C terminus and the quencher DABCYL at the N terminus (AnaSpec, Fremont, CA, USA), according to manufacturer's procedure. Fluorescence was monitored with a Fluostar Galaxy microplate fluorimeter (BMFG Labtechnologies, Offenburg, Germany).

MS/MS sequencing of proteolytic fragments of cyclic peptide

Purified cyclic GG-Hst1-LPET was subjected to trypsin digestion. The peptides generated from proteolytic digestion were extracted and concentrated for analysis by RP-HPLC and tandem MS. RP-HPLC was carried out with a Waters NanoAcquity HPLC system with a flow rate of 250 nl/min and mobile phases of 0.1% formic acid in water and 0.1% formic acid in acetonitrile. After elution with 1% acetonitrile for 1 min, a gradient was applied with an increase of 2% acetonitrile per minute to 40% acetonitrile. The analytical column was 0.075 μm × 10 cm with the tip pulled to 0.005 μm and

self-packed with 3 μm Jupiter C18 (Phenomenex). The column was interfaced to a Thermo LTQ linear ion-trap mass spectrometer in a nanospray configuration, and data were collected in full scan mode followed by MS/MS analysis in a data-dependent manner.

CD spectroscopy

CD spectra were collected for GG-Hst1-LPETGG and cGG-Hst1-LPET with a Jasco J-810 spectropolarimeter (Jasco Inc., Easton, MD, USA). All spectra were collected at room temperature between 200 and 260 nm at a scan rate of 100 nm/min with the bandwidth set to 1 nm and the response set to 0.5 s. The final spectrum was the accumulated average of 10 scans. The 50 μM peptide samples were measured in buffer (25 mM sodium phosphate buffer, pH 7.4) and 30 mM SDS. These samples were also prepared in the presence of 100 μM $ZnCl_2$. A 2,2,2-trifluorethanol (TFE) titration was performed on peptide samples at TFE concentrations of 10, 20, 30, 40, and 50% (v/v). A blank spectrum, for a solution without peptide, was collected for each sample and subtracted in the final analysis.

NMR spectroscopy

Aqueous samples of GG-Hst1-LPETGG and cGG-Hst1-LPET were prepared by dissolving 1 mg of lyophilized peptide in 500 μl of 90% H_2O:10% D_2O. 2D ^1H-NOESY spectra (Bruker pulse program noesyesgpph) were recorded for each sample on a Bruker Avance 600 MHz spectrometer (Bruker, Billerica, MA, USA) using a mixing time of 100 ms. Spectra were acquired with 4096×512 data points in the F2 and F1 dimensions, respectively, at a spectral width of 8503.401 Hz. Following data acquisition, SDS-$d25$ (Cambridge Isotopes Laboratory, Andover, MA, USA) was added to each sample to a final detergent concentration of 200 mM, and NOESY spectra were acquired. All samples were adjusted to pH 4–4.5, and 4,4-dimethyl-4-silapentane-1-sulfonic acid was added as an internal chemical shift standard. All spectra were recorded at 298 K.

In vitro wound closure assay

In vitro wound closure experiments were performed in 48-well culture plates (Greiner-Bio-One, Alphen a/d Rijn, The Netherlands) with human buccal epithelial cells (HO-1-N-1; provided by the Japanese Collection of Research Bioresources, Osaka, Japan). With a sterile tip, a scratch was made in a confluent layer of cells that were serum deprived in DMEM/F12 culture medium (Invitrogen, Carlsbad, CA, USA) for 6 h. The width of the scratch was measured at the beginning and after 18 h of culture on microscopic images (Leica DM IL, Leica DFC320 camera; Leica Microsystems, Wetzlar, Germany). Relative closure was calculated by dividing the closure in the presence of peptide by that in the absence of peptide. Final concentrations of synthetic peptides in the assays varied between 0.1 nM and 10 μM as indicated. As a positive control, 10 ng/ml rhEGF (Invitrogen) was used.

Peptide-binding assay

Peptide binding to the cell was studied using HeLa cells. Cells at a density of 10^6 cells/ml were incubated with 10 nM or 10 μM of peptides at 4°C to prevent intracellular uptake of peptides. After 1 h, cells were lysed in 50 mM Tris and 150 mM NaCl containing 1% SDS. The lysate was incubated with 20 μl streptavidin-agarose beads for 30 min at room temperature, and biotin-containing peptides were precipitated, washed 3 times with PBS containing 0.1% Tween-20 (PBS-T), and boiled in SDS-PAGE loading buffer. Samples were sepa-

rated on a 12% Tris-Tricine gel, blotted onto nitrocellulose, and blocked with PBS-T supplemented with 5% BSA for 30 min. After being washed, the blots were probed with streptavidin-horseradish peroxidase for 30 min. Detection was accomplished with an ECL detection kit.

RESULTS

SrtA-catalyzed cyclization of Hst1 is more efficient than organic chemical cyclization

Using standard Fmoc chemistry, we synthesized a linear peptide consisting of a discontinuous sequence of Hst1 starting with an orthogonally protected Glu-loaded resin that allowed on-resin head-to-tail ligation (**Fig. 1***A*). Synthesized material cleaved from the resin was fractionated by RP-HLC (Fig. 1*B*). Then, fractions were analyzed by MALDI-TOF MS to identify the linear and cyclic peptide. Both peptides were purified from the crude material (Fig. 1*C, D*) with an overall yield between 1 and 3%.

Because of the low yields, we exploited the applicability of SrtA to catalyze cyclization (**Fig. 2***A*). Fmoc chemistry was used to synthesize a linear Hst1 variant equipped with the sortase recognition motif LPETGG at the C terminus and a GG motif at the N terminus (GG-Hst1-LPETGG). Then, we incubated 150 μM of this peptide with 50 μM recombinant SrtA in sortase reaction buffer and monitored the reaction by RP-HPLC (Fig. 2*B*) and SDS-PAGE (Fig. 2*C*). After 21 h, the linear peptide GG-Hst1-LPETGG was converted into the cyclic product, with no input material remaining. ESI-MS analysis of the RP-HPLC peak fraction
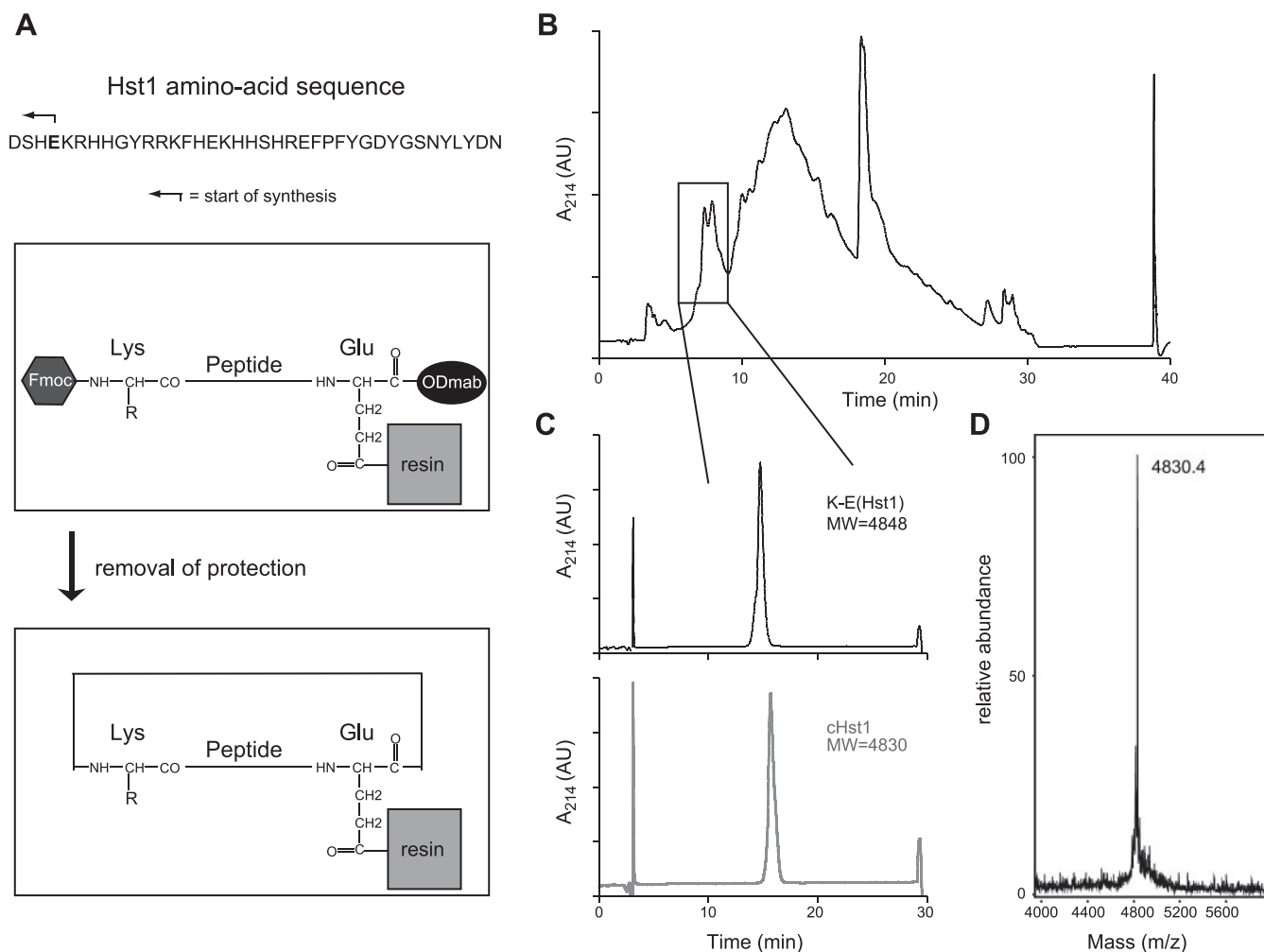

Figure 1. Chemical cyclization of Hst1. *A*) Glutamic acid at position 4 was used as starting point for peptide synthesis using an orthogonally protected Glu-loaded resin [Fmoc-Glu(Wang-resin)-ODmab] that allowed on-resin head-to-tail ligation after completion of the discontinuous sequence (K^5-N^{38})(D^1-E^4) in short K-E(Hst1). *B*) RP-HPLC profile after synthesis. Fractions depicted in the box were collected and further purified. Material eluting at longer retention times included all kinds of byproducts; MS analysis revealed large constructs, probably dimers and trimers. *C*) Purified fractions showed a single peak in their respective RP-HPLC profiles after rechromatography on an analytical column. Linear Hst1 has a slightly shorter retention time than cHst1. The loss of a positively charged N terminus and a negatively charged C terminus on cyclization by lactam-bond formation results in a slightly more hydrophobic character of the cyclic variant. Identities of these peaks were confirmed by MALDI-TOF. *D*) MALDI-TOF analysis of cHst1 revealed a molecular mass corresponding to linear Hst1 minus a molecule of water, indicative for the formation of a lactam bond between E^4 and K^5. AU, arbitrary units.
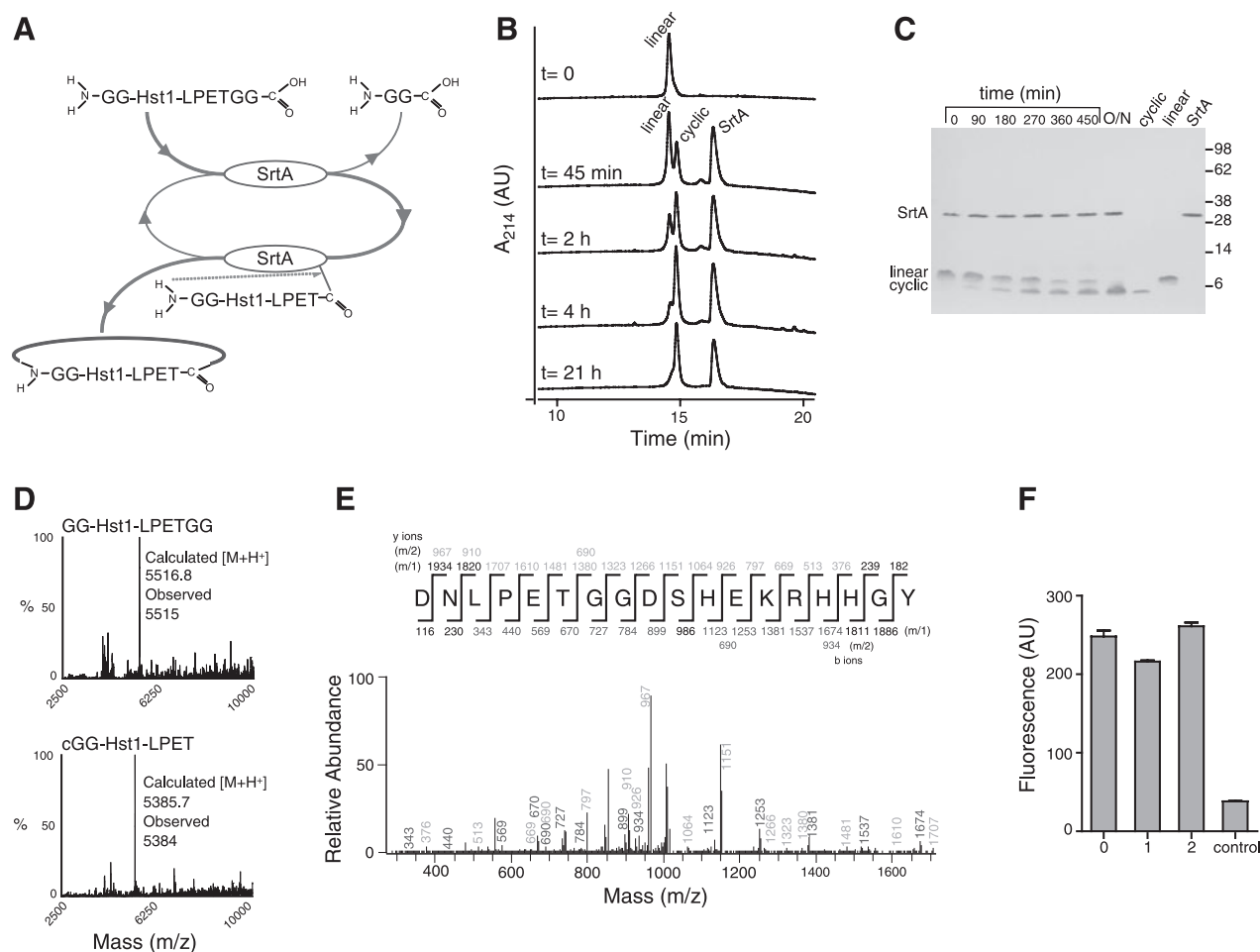
Figure 2. SrtA-catalyzed cyclization of GG-Hst1-LPETGG. *A*) Schematic illustration of the enzymatic cyclization reaction. *B*) Progression of the reaction as monitored by RP-HPLC. *C*) Progression of the as monitored by SDS-PAGE. Coomassie-stained gel shows the cyclization at indicated time points. Control lanes on the right-hand side of the gel show purified cyclic peptide cGG-Hst1-LPET (cHst), linear peptide GG-Hst1-LPETGG (Hst), and SrtA. *D*) ESI-MS analysis of RP-HPLC fractions containing GG-Hst1-LPETGG and cGG-Hst1-LPET, respectively. Difference in mass corresponds to calculated differences between cyclic and linear versions, *i.e.*, 231 Da, corresponding to the removal of GG and 1 molecule of water. *E*) MS/MS spectrum of a tryptic fragment of cyclic GG-Hst1-LPET showing the ligation of the N-terminal residues (GGDSHEK) to the C-terminal LPET motif. Expected masses for y and b ions are listed above and below the peptide sequence. Ions that were positively identified in the MS/MS spectrum are indicated. The most prominent daughter ions are indicated in the MS/MS spectrum. *F*) SrtA activity measured with FRET peptide-substrate. Reactions were performed in sortase reaction buffer for 1 h at 37°C and analyzed fluorometrically by using 350 nm for excitation and 490 nm for recordings. 0: SrtA activity before use. 1: Specific activity of SrtA after 1 cyclization and RP-HPLC purification cycle. 2: Specific activity of SrtA after 2 cyclization and purification cycles. Control: no enzyme.

showed the presence of a single species with a molecular mass corresponding to that of the cyclic peptide cGG-Hst1-LPET (Fig. 2*D*). MS/MS analysis after tryptic digestion showed the presence of the fragment DN*LPETGG*DSHEKRHHGY, confirming that transpeptidation between the C-terminal *LPET* and the N-terminal *GG* motif had been accomplished (Fig. 2*E*).

Both the cyclic reaction product and the enzyme could be purified from the reaction mixture in a simple and efficient manner using semipreparative RP-HPLC (Fig. 2*B*). Fractions containing the cyclic peptide cGG-Hst1-LPET and SrtA were separately pooled and lyophilized. After reconstitution of the SrtA in sortase reaction buffer, the activity was determined using the fluorogenic SrtA substrate I dabcyl-LPETG-Edans (Fig.

2*F*). The activity was fully retained, even after 3 HPLC/lyophilization cycles. In this manner, a single batch of SrtA could be reused several times, increasing the ease and efficiency of the method.

Biological activity of SrtA-cyclized peptide cGG-Hst1-LPET

After purification, the biological activity of cGG-Hst1-LPET was evaluated in an artificial wound model (**Fig. 3***A*). Maximal stimulation of wound closure occurred at ~10 nM cGG-Hst1-LPET, comparable to that of cHst1 produced by organic chemical ligation and ~1000 times lower than the equipotent concentrations of the linear parent peptides GG-Hst1-LPETGG and Hst1, respectively (Fig. 3*B–D*). The
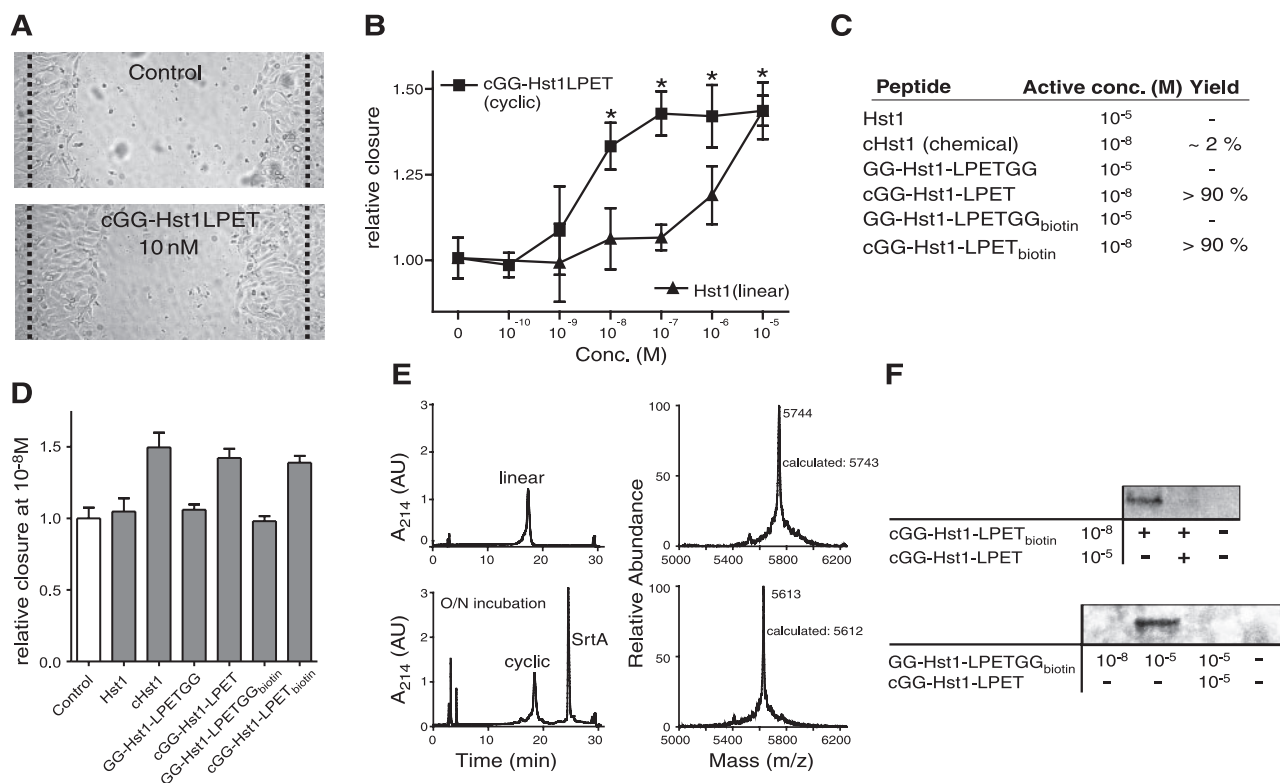
Figure 3. Wound closure-promoting activity and binding affinity of linear Hst1 and the cyclic peptide cGG-Hst1-LPET. *A*) Micrographs of scratch assays with confluent layers of HO-1-N-1 cells. Wounds (scratches) were treated with and without 10 nM cGG-Hst1-LPET for 18 h. Dotted lines indicate the borders of the wounds before incubation. *B*) Dose-response curves of wound closure experiments comparing Hst1 and cGG-Hst1LPET. Each point represents the mean $\pm$ SD of 3 experiments as shown in *A*, carried out in 6-fold. $*P < 0.05$. *C*) Minimal concentrations of the peptides needed for maximal wound closure activity, as determined in the scratch assay, and the yield of cyclization of the different peptides deduced from RP-HPLC profiles. *D*) *In vitro* wound closure activity of the different peptides at a concentration of 10^{-8} M. All 3 forms of cyclic peptides showed increased wound closure in comparison to the linear peptides. *E*) SrtA-catalyzed cyclization of Hst1, biotinylated at K^{17}. RP-HPLC profile of linear GG-Hst1-LPETGG$_{biotin}$ (top left panel) and of the reaction mixture of this peptide after overnight incubation with SrtA (bottom left panel), showing the conversion to cGG-Hst1-LPET$_{biotin}$. MALDI-TOF analysis identified the respective peaks as GG-Hst1$_{biotin}$-LPETGG (top right panel) and cGG-Hst1-LPET$_{biotin}$ (bottom right panel). Difference in mass corresponds to calculated differences between cyclic and linear versions, *i.e.*, 231 Da, corresponding to the removal of GG and 1 molecule of water. *F*) HeLa cells were incubated with the linear GG-Hst1-LPETGG$_{biotin}$ and the cyclic cGG-Hst1-LPET$_{biotin}$ at 4°C to prevent intracellular uptake of peptides. Following lysis, cell lysates were immunoblotted with avidin-peroxidase to detect biotinylated peptides. Top: binding of cGG-Hst1-LPET$_{biotin}$ to HeLa cells at a concentration of 10^{-8} M of peptide. This binding was abolished in the presence of 10^{-5} M cGG-Hst1-LPET. Bottom: no binding of the linear peptide GG-Hst1-LPETGG$_{biotin}$ to HeLa cells at a concentration of 10^{-8} M; a concentration of 10^{-5} M was needed for binding. This binding was abolished in the presence of 10^{-5} M cGG-Hst1-LPET.

presence of the SrtA motifs did not adversely affect the cell-activating properties of the linear or the cyclic variant.

We next examined whether the increase in activity of cGG-Hst1-LPET was accompanied by an increased affinity for its cellular receptor, the identity of which remains to be established. To enable sensitive detection in binding assays, we prepared a biotinylated cyclic variant by overnight incubation of chemically synthesized GG-Hst1-LPETGG, biotin-tagged at K^{17}, with SrtA. Within 16 h, this biotinylated peptide was completely converted to the cyclic cGG-Hst1-LPET$_{biotin}$, as indicated by RP-HPLC and confirmed by MALDI-TOF analysis (Fig. 3*E*). The wound closure stimulating activity of this variant was comparable to that of the nonbiotinylated variant (Fig. 3*C*, *D*). HeLa cells were incubated with the linear GG-Hst1-LPETGG$_{biotin}$ and the cyclic cGG-Hst1-LPET$_{biotin}$ at 4°C to prevent intracellular uptake of peptides. Following lysis, cell lysates were immunoblotted with avidin peroxidase to detect biotinylated peptides (Fig. 3*F*). At 10 nM concentration, only binding of cyclic cGG-Hst1-LPET$_{biotin}$, but not of linear GG-Hst1-LPETGG$_{biotin}$, was detected. Binding of cyclic cGG-Hst1-LPET$_{biotin}$ was blocked when incubation was conducted in the presence of 10 μM unlabeled cGG-Hst1-LPET, indicating that it was not mediated by the biotin moiety of the peptide. Binding of linear biotinylated GG-Hst1-LPETGG$_{biotin}$ was only detected at a concentration of 10 μM. Coincubation with 10 μM cyclic cGG-Hst1-LPET completely abolished the binding of the linear peptide, suggesting that the cyclic and the linear variants compete for the same receptor. Overall the results of these experiments suggest that cyclization of Hst1 increases its affinity for the receptor.
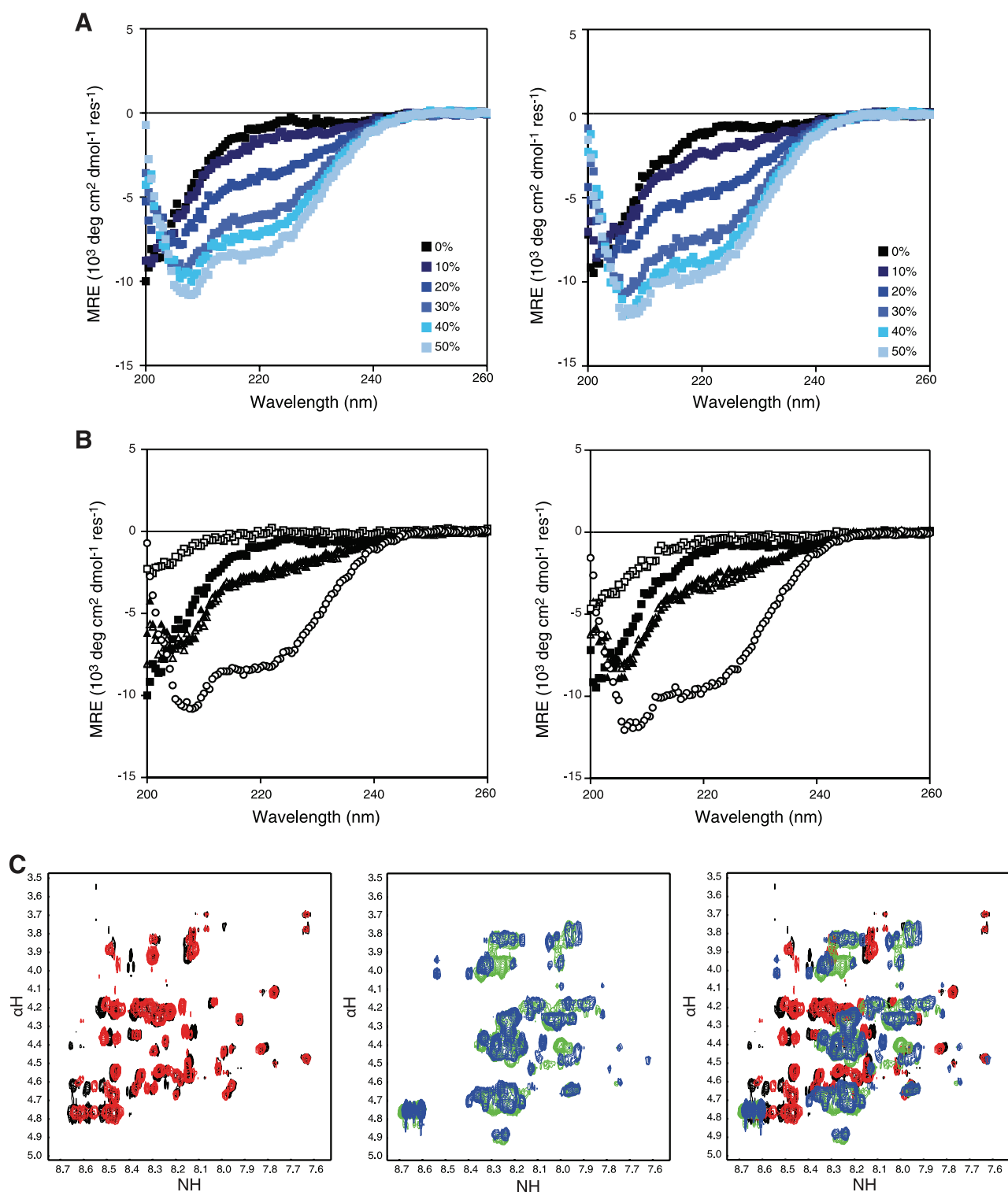
Figure 4. CD and NMR spectroscopy of the linear GG-Hst1-LPETGG and cyclic cGG-Hst1-LPET. *A*) Effect of increasing TFE concentration on the structure of GG-Hst1-LPETGG and cGG-Hst1-LPET. Percentage volume of TFE added to each 50 μM peptide sample is indicated. *B*) Effect of Zn^{2+} on the structure of GG-Hst1-LPETGG and cGG-Hst1-LPET. CD spectra were recorded in buffer (■), and in buffer in the presence of either of the following additives: 100 μM Zn^{2+} (□); 30 mM SDS (▲); 30 mM SDS with 100 μM Zn^{2+} (△); and 50% (v/v) 2,2,2-trifluoroethanol (TFE; ○). *C*) NH-αH fingerprint region from the 2D ¹H-NOESY spectra of GG-Hst1-LPETGG and cGG-Hst1-LPET. Left: spectra of GG-Hst1-LPETGG (black) superimposed on cGG-Hst1-LPET (red) in aqueous solution. Middle: spectra of GG-Hst1-LPETGG (blue) and cGG-Hst1-LPET (green) in the presence of SDS micelles. Right: comparison of all of the spectra (coloring scheme as above).

Structural analysis

To examine the structural properties of the linear and cyclic peptides, we conducted a conformational analysis using CD (**Fig. 4A, B**) and NMR spectroscopy (Fig. 4*C*). The effects of the cosolvent TFE, binding of Hst1 peptides to SDS micelles, and the addition of Zn^{2+} were investigated here, as earlier studies have shown that these conditions induced some structure in the related histatin 3 and histatin 5 peptides and/or improved their antimicrobial activity (15–17). Both peptides GG-Hst1-LPETGG and cGG-Hst1-LPET can adopt α-helical conformations, as seen by the emergence of strong negative mean residue ellipticity (MRE) values at 208 and 222 nm at increasing TFE concentrations (Fig. 4*A*). The dependence of the structural change on the TFE concentration was identical for both peptides, indicating that the propensity to form a helical structure has not been altered by the cyclization. Also, both peptides similarly showed a decrease in MRE in the presence of 100 μM Zn^{2+}, likely due to peptide aggregation, since these samples became turbid with the addition of zinc ions (Fig. 4*B*). SDS micelles prevented Zn^{2+}-induced peptide aggregation of the linear peptide equally well as the cyclic peptide, since the spectra of 30 mM SDS with 100 μM Zn^{2+} were identical to that of the SDS-bound peptide in both cases, and these solutions remained clear (Fig. 4*B*). The NH-αH fingerprint region from the 2D ^{1}H-NOESY spectra of GG-Hst1-LPETGG superimposed on cGG-Hst1-LPET in aqueous solution revealed a similar conformation for both peptides, with only a few shifted peaks (Fig. 4*C*, left panel). In the presence of SDS micelles, the slight differences indicate that the 2 micelle-bound peptides adopt equivalent structures (Fig. 4*C*, middle panel). The shifted peaks between the spectra are likely due to the presence of the cyclized backbone and do not indicate a large conformational change between the peptides. A comparison of all of the spectra reveals that the conformation of the peptide is more dependent on the solvent conditions used rather than the nature of the peptide present in the sample (Fig. 4*C*, right panel).

DISCUSSION

Cyclic peptides are highly valued tools in biomedical research, because they often show higher receptor affinity, enhanced biological activity, and improved serum stability compared with their linear counterparts. Fundamental and applied research in this field, however, are hampered by the fact that current cyclization methods are inefficient for cyclization of large peptides (>10 residues) and exhibit considerable variation in cyclization yield with respect to sequence of linear precursor. In this study, we describe a novel, simple method for efficient manufacturing of cyclic peptides, using the *S. aureus* enzyme SrtA. The method is robust and has high yield (Fig. 2). Moreover, it is technically simple and can be conducted with standard biochemical equipment, making it accessible for biomedical researchers without expert skills in organic chemical synthesis. Using this method, we have up to now cyclized successfully >14 different peptides, ranging in length from 15 to 45 residues (unpublished results).

A possible limitation of the described method is that peptides must be extended with the LPETGG and GG sequences in order to be converted by sortase. In case of Hst1, this proved not to be a major problem, since both the linear and the cyclic elongated variants were as active as the original peptides (Figs. 2 and 3). This indicates that the active domain is not located in the N or C terminus of Hst1, corroborating previous studies showing that N- and C-terminal truncation did not abolish the biological activity (3, 4).

We found that on cyclization of Hst 1, both its biological activity and its affinity for its receptor drastically increased, in line with the hypothesis that cyclization stabilizes the bioactive, receptor-binding conformation of the peptide. However, structural analysis using CD and NMR spectroscopy could not find any evidence for our initial assumption that cyclic GG-Hst1-LPET in solution has a more constrained structure than its linear counterpart. Likewise, recent studies of short Trp-rich antimicrobial peptides showed that cyclic 11-mer peptides did not have a fixed backbone structure, in contrast to related cyclic 6-mer peptides (2). The lack of order in the solution structure of both linear and cyclic histatin suggests that the transition to the bioactive conformation takes place after initial binding to its receptor. This scenario favors the induced-fit model of ligand-receptor activation, in which the ligand adopts its bioactive conformation only after initial (weak) binding to its receptor (18). We hypothesize that the increased structural constraint imposed on histatin by cyclization only becomes manifest when the peptide is situated in the ligand-binding region of the receptor. FJ

REFERENCES

1. Cascales, L., and Craik, D. J. (2010) Naturally occurring circular proteins: distribution, biosynthesis and evolution. *Org. Biomol. Chem.* **8,** 5035–5047
2. Nguyen, L. T., Chau, J. K., Perry, N. A., de Boer, L., Zaat, S. A. J., and Vogel, H. J. (2010) Serum stabilities of short tryptophan- and arginine-rich antimicrobial peptide analogs. *PLoS One* **5,** e12684
3. Oudhoff, M. J., Bolscher, J. G. M., Nazmi, K., Kalay, H., van't Hof, W., Nieuw Amerongen, A. V., and Veerman, E. C. I. (2008) Histatins are the major wound-closure stimulating factors in human saliva as identified in a cell culture assay. *FASEB J.* **22,** 3805–3812
4. Oudhoff, M. J., Kroeze, K. L., Nazmi, K., van den Keijbus, P. A. M., van't Hof, W., Fernandez-Borja, M., Hordijk, P. L., Gibbs, S., Bolscher, J. G. M., and Veerman, E. C. I. (2009) Structure-activity analysis of histatin, a potent wound healing

peptide from human saliva: cyclization of histatin potentiates molar activity 1000-fold. *FASEB J.* **23,** 3928–3935

5. Tsukiji, S., and Nagamune, T. (2009) Sortase-mediated ligation: a gift from gram-positive bacteria to protein engineering. *Chem. Bio. Chem.* **10,** 787–798

6. Proft, T. (2010) Sortase-mediated protein ligation: an emerging bio/technology tool for protein modification and immobilisation. *Biotechnol. Lett.* **32,** 1–10

7. Popp, M. W., Antos, J. M., Grotenbreg, G. M., Spooner, E., and Ploegh, H. L. (2007) Sortagging: a versatile method for protein labeling. *Nat. Chem. Biol.* **3,** 707–708

8. Antos, J. M., Chew, G. L., Guimaraes, C. P., Yoder, N. C., Grotenbreg, G. M., Popp, M. W., and Ploegh, H. L. (2009) Site-specific N- and C-terminal labeling of a single polypeptide using sortases of different specificity. *J. Am. Chem. Soc.* **131,** 10800–10801

9. Antos, J.M., Popp, M.W., Ernst, R., Chew, G.L., Spooner, E., and Ploegh, H. L. (2009) A straight path to circular proteins. *J. Biol. Chem.* **284**, 16028–16036

10. Popp, M.W., Dougan, S.K., Chuang, T.-Y., Spooner, E., and Ploegh, H. L. (2011) Sortase-catalyzed transformation that improve the properties of cytokines. *Proc. Natl. Acad. Sci. U. S. A.* **108,** 3169–3174

11. Ton-That, H., Liu, G., Mazmanian, S. K., Faull, K. F., and Schneewind, O. (1999) Purification and characterization of sortase, the transpeptidase that cleaves surface proteins of *Staphylococcus aureus* at the LPXTG motif. *Proc. Natl. Acad. Sci. U. S. A.* **96,** 12424–12429

12. Pritz, S., Wolf, Y., Kraetke, O., Klose, J., Bienert, M., and Beyermann, M. (2007) Synthesis of biologically active peptide nucleic acid-peptide conjugates by sortase-mediated ligation. *J. Org. Chem.* **72,** 3909–3912

13. Tanaka, T., Yamamoto, T., Tsukiji, S., and Nagamune, T. (2008) Site-specific protein modification on living cells catalyzed by sortase. *Chem. Bio. Chem.* **9,** 802–807

14. Navarre, W. W., and Schneewind, O. (1999) Surface proteins of gram-positive bacteria and mechanisms of their targeting to the cell wall envelope. *Microbiol. Mol. Biol. Rev.* **63,** 174–229

15. Brewer, D., and Lajoie, G. (2002) Structure-based design of potent histatin analogues. *Biochemistry* **41,** 5526–5536

16. Melino, S., Rufini, S., Sette, M., Morero, R., Grottesi, A., Paci, M., and Petruzzelli, R. (1999) Zn(2+) ions selectively induce antimicrobial salivary peptide histatin-5 to fuse negatively charged vesicles. Identification and characterization of a zinc-binding motif present in the functional domain. *Biochemistry* **38,** 9626–9633

17. Rydengård, V., Andersson Nordahl, E., and Schmidtchen, A. (2006) Zinc potentiates the antibacterial effects of histidine-rich peptides against *Enterococcus faecalis*. *FEBS J.* **273,** 2399–2406

18. Zhou, H. X. (2010) From induced fit to conformational selection: a continuum of binding mechanism controlled by the timescale of conformational transitions. *Biophys. J.* **98,** L15–L17